Behavioural Brain Research 281 (2015) 69–77

Contents lists available at ScienceDirect

Behavioural Brain Research

journal homepage: www.elsevier.com/locate/bbr

Research report

TRPC3 channels critically regulate hippocampal excitability and contextual fear memory

Sarah M. Neuner[a], Lynda A. Wilmott[a], Kevin A. Hope[a], Brian Hoffmann[b], Jayhong A. Chong[c], Joel Abramowitz[d], Lutz Birnbaumer[d], Kristen M. O'Connell[e], Andrew K. Tryba[f], Andrew S. Greene[b,g], C. Savio Chan[h], Catherine C. Kaczorowski[a,*]

[a] Department of Anatomy and Neurobiology, The University of Tennessee Health Science Center, Memphis, TN, United States
[b] Department of Biotechnology and Bioengineering, Medical College of Wisconsin, Milwaukee, WI, United States
[c] Hydra Biosciences, Cambridge, MA, United States
[d] Laboratory of Neurobiology, National Institute of Environmental Health Sciences, Research Triangle Park, NC, United States
[e] Department of Physiology, The University of Tennessee Health Science Center, Memphis, TN, United States
[f] Department of Pediatrics, The University of Chicago, Chicago, IL, United States
[g] Department of Physiology, Medical College of Wisconsin, Milwaukee, WI, United States
[h] Department of Physiology, Northwestern Fienberg School of Medicine, Chicago, IL, United States

HIGHLIGHTS

- Targeted proteomics identify set of proteins correlated with contextual fear memory.
- Whole-genome transcript profiling highlights *Trpc3* as putative regulator of memory.
- Mechanistic studies demonstrate TRPC3 regulates hippocampal neuronal excitability.
- Functional studies show TRPC3 regulates contextual fear memory *in vivo*.

GRAPHICAL ABSTRACT

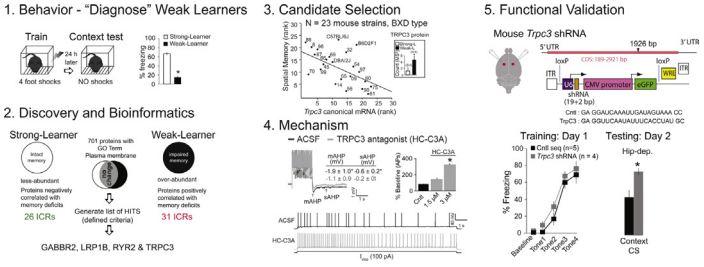

ARTICLE INFO

Article history:
Received 5 December 2014
Accepted 8 December 2014
Available online 13 December 2014

Keywords:
Hippocampus
Memory
Transient receptor potential cation channel
Afterhyperpoloarization
Aging
Proteomics

ABSTRACT

Memory formation requires *de novo* protein synthesis, and memory disorders may result from misregulated synthesis of critical proteins that remain largely unidentified. Plasma membrane ion channels and receptors are likely candidates given their role in regulating neuron excitability, a candidate memory mechanism. Here we conduct targeted molecular monitoring and quantitation of hippocampal plasma membrane proteins from mice with intact or impaired contextual fear memory to identify putative candidates. Here we report contextual fear memory deficits correspond to increased *Trpc3* gene and protein expression, and demonstrate TRPC3 regulates hippocampal neuron excitability associated with memory function. These data provide a mechanistic explanation for enhanced contextual fear memory reported herein following knockdown of TRPC3 in hippocampus. Collectively, TRPC3 modulates memory and may be a feasible target to enhance memory and treat memory disorders.

© 2014 The Authors. Published by Elsevier B.V. This is an open access article under the CC BY-NC-ND license (http://creativecommons.org/licenses/by-nc-nd/3.0/).

1. Introduction

Protein synthesis [1–3], and perhaps protein degradation [4], is required for memory formation yet the specific proteins necessary remain largely unknown. Determination of the molecular

* Corresponding author. Tel.: +1 9014482178; fax: +1 9014487193.
E-mail address: ckaczoro@tennessee.edu (C.C. Kaczorowski).

http://dx.doi.org/10.1016/j.bbr.2014.12.018
0166-4328/© 2014 The Authors. Published by Elsevier B.V. This is an open access article under the CC BY-NC-ND license (http://creativecommons.org/licenses/by-nc-nd/3.0/).

mechanisms that underlie the cellular changes involved in memory formation and storage is critical for the understanding of these complex processes and the development of novel therapeutic approaches. Recent work has identified cellular excitability changes that correspond to the formation of hippocampus-dependent memories [5–7]. In this regard, we previously identified changes in neuronal excitability specifically associated with the onset of age-related contextual fear memory deficits in mice [8]. Given that ion channels and receptors (ICRs) are known to govern neuron excitability and plasticity [6,9], we hypothesize that these excitability changes reflect alterations in the synthesis and/or degradation of specific ICRs that, in turn, play a critical role in memory function.

To identify novel candidate proteins that play a critical role in memory, we developed a targeted proteomics approach to identify lead-candidate ICR proteins. Specifically, the hippocampus plasma membrane proteome of mice exhibiting intact contextual fear memory was compared to that of age-matched controls exhibiting impaired memory. ICRs that were differentially expressed relative to memory performance were identified and prioritized for further studies using sophisticated data mining strategies, including network and pathway analysis [10] and transcript profiling across a genetically diverse panel of mice [11–14]. Subsequent functional validation of our top candidate, transient potential canonical chancel 3 (TRPC3), was carried out using Western blot, electrophysiology, viral-mediated gene knockdown technology, and behavioral assays. Here, select downregulation of TRPC3 in the hippocampus exposed its novel role in regulating neuron excitability and *enhancement* of contextual fear memory.

2. Methods

2.1. Animals

Mice used in this study include: (1) C57Bl6J/SJL for proteomics analysis, (2) BXD recombinant inbred strains from C57Bl6J and DBA2J founders for population-based transcript profiling, (3) Trpc3−/− KO mice that were generated on a 129Sv background [15] and corresponding Sv129 littermates were used as wild-type controls, and (4) C57Bl6J for subsequent AAV9-shRNA *Trpc3* validation studies (unless otherwise noted). All mice were group housed (2–5 per cage) and maintained in colony-housing (12-hour light/dark cycle) with *ad libitum* access to food and water in accordance with approval by the Medical College of Wisconsin Animal Care and Use Committee and the University of Tennessee Health Science Center Animal Care and Use Committee. All animals were naïve prior to use. Males were used exclusively except when using BXD mice [11–14], where the quantity of mice was limited. One animal from the present study was excluded from the viral-mediated gene knockdown portion of the study based on meeting exclusion criteria established prior to data collection; behavioral freezing >3 SD away from the group mean measured on 2 independent memory tests (hippocampus and amygdala-dependent).

2.2. Behavioral assays

All mice were transported for at least three days prior to behavioral assays to allow time for habituation to transfer. After habituation to transport, mice were trained on either a standard contextual or delay fear conditioning (FC) paradigm. Contextual fear memory, which is known to be hippocampus-dependent [16], was tested 24 h later over 10 min (unless otherwise noted). Delay conditioning consisted of a 90–180 s baseline period followed by 4 pairings of a tone (20 s, 80 dB) that precedes and coterminates with a mild shock (1 s, 0.9 mA) separated by ~210 s. Standard contextual fear conditioning consisted of an identical protocol but in the absence of a tone. Behavioral freezing, an index of conditioned fear, was assessed for 10 min (unless noted otherwise) using Freeze Frame software (Coulbourn Instruments, PA). A subset of mice were trained on an immediate shock deficit (ISD) paradigm where mice received shock but were removed from the training chamber prior to forming an association between the context and the shock. This group served as control for protein changes that result from exposure to shock. ISD mice were placed in the conditioning chamber for 5 s, received a single foot shock (0.9 mA, 4 s) matched to the cumulative sum of foot shocks in FC group, and returned to the home cage within 30 s. Contextual memory tests 24 h later indicated little to no contextual fear memory was formed in ISD compared to FC mice. Immediately following memory tests, mice were anesthetized using isoflurane and decapitated for fresh, snap frozen, and/or fixed tissue collection.

2.3. Protein analytics

To maximize identification of non-redundant plasma membrane ICRs for proteomics, the hippocampus ($n = 4$ mice/grp) was freshly dissected, enriched for membrane proteins, and processed using filter-assisted sample preparation [17]. Prior analysis of the hippocampus membrane proteome by Mann and colleagues suggests a total of 12 LC-runs (240 min gradients) comprised of 4 mice per group (3 technical replicates per mouse) provides substantial and reliable coverage of the hippocampus membrane proteome including ion channels and receptors [17]. Identical methods were used herein, including $n = 4$ mice/grp and 3 technical replicates per mouse, with the exception that we performed membrane enrichment steps on fresh rather than frozen hippocampus and we increased the LC gradient to 310 min to increase coverage of the hippocampus proteome. Tryptic peptides (1.9 μL/run) were acidified to pH 3–4 and passed over C18 resin (particle size 5 μm; Phenomenex, CA) packed 10 cm column (inner diameter of 50 μM) coupled to a NanoAccuity UPLC system (Waters, MA). A 310 min customized reverse phase liquid chromatography gradient from buffer A to buffer B (98% ACN, 1.9% HPLC H_2O, 0.1% FA) was increased linearly from initial conditions 2% (>20 min), 3 min/2%, 5 min/10%, 190 min/30%, 65 min/65%, 5 min/75%, 5 min/98%, 30 min/2%). Electrospray ionization of eluted peptides was analyzed on LTQ-Orbitrap Velos Mass Spectrometer (Thermo Scientific, Waltham, MA). Peaks were extracted using Extract MSn 5.0 [18], and searched using Mascot and Sequest algorithms against the UnitProtKB mouse database (32,271 proteins). Modifications for oxidation of methionine (+16-Da), alkylation of cysteine (+57-Da), acetylation of N-terminus (+42-Da), and up to 2 missed cleavages (K, R) were allowed. The precursor tolerance was set at 1.4 amu. Visualize Software was used for quantitative analyses of the hippocampus plasma membrane proteome of mice exhibiting impaired relative to intact memory ($n = 4$ mice/grp) as described [19,20]. In a single hippocampus, analyses with 5-h gradient (3 technical replicates) identified a total of 701 proteins annotated as 'plasma membrane' using GO term [21] with at least two identified peptides ($\geq$2 ms^2 scans) per protein, and were identified in $\geq$3 of 4 mice per group. Differential protein abundances were detected by quantifying the number of spectra observed for each protein, and defined as proteins with >20% abundance difference between mice with impaired relative to intact contextual fear memory. Fifty-seven plasma membrane proteins were differentially expressed ICRs based on established criteria. Bioinformatics and variation in gene expression relative to contextual fear memory status in a murine genetic reference panel [14] were used to prioritize candidates for functional studies (see below).

Western blots were performed from whole hippocampal lysates according to established procedures [22,23] unless otherwise

Table 1
Trpc expression relative to performance on hippocampus-dependent contextual fear task (Trait: 11011).

Gene	Probe set	Mean expression	Rho, Spearman rank	*p*-value (*N* = 23 BXD strains)
Trpc1	5409349	12.91	0.092	0.680
Trpc2	5330076	10.91	0.051	0.818
Trpc3	**5158157**	**10.52**	**−0.577**	**0.003**[a]
Trpc4	4719862	11.87	−0.089	0.690
Trpc5	5280284	11.78	−0.158	0.476
Trpc6	5329270	12.06	0.169	0.446
Trpc7	5138509	9.22	−0.114	0.610

[a] Cutoff for 95% confidence interval corrected for multiple comparisons: $p \leq 0.007$.

noted. Brains were removed, the hippocampus dissected and immediately snap frozen in liquid nitrogen and stored at −80 until further use. Samples were removed from −80, placed in lysis buffer (0.32 M sucrose, 3 mM HEPES, pH 7.4 plus Roche miniComplete protease inhibitor cocktail), and kept on ice throughout the procedure. For experiments conducted to validate results from proteomics analysis, samples were first enriched for membrane proteins using established methods [17] prior to being placed in lysis buffer. Samples were homogenized by sonication and protein concentration was determined using a BCA Assay (Pierce) or Nanodrop2000 Spectophotometer (Thermo Scientific). Sample (15–20 μg protein) was loaded and separated on a 10% SDS-PAGE gel. Proteins were transferred using the Bio-Rad TurboTransfer system and blocked for 30 min at room temperature. Primary antibodies for TRPC3, GluR2, NR2B, or NR1 (#ACC-016, Alamone Labs, #75-002, #75-097, NeuroMab, and #G8913, Sigma, 1:1000–1,5000, respectively) were followed by the appropriate peroxidase-conjugated secondary antibody (HRP anti-rabbit or anti-mouse, PI-1000/PI-2000, Vector Labs, 1:1000–1:5000). Bands were visualized using the SuperSignal West Pico Chemiluminescent Substrate kit (Pierce) and ChemiDoc system from BioRad and quantified using NIH ImageJ Software. GAPDH (#10R-G109a, Fitzgerald, 1:5000) was used as a loading control. In cases where samples had been enriched for membrane proteins and GAPDH was not present, Ponceu S staining was used as a loading control according to established methods [24].

2.4. Bioinformatics

Bioinformatic pathway analysis software Ingenuity Pathway Analysis (IPA®, www.ingenuity.com) was used to identify gene/protein networks that were differentially enriched in samples relative to memory status. Only direct molecular interactions within gene/protein pathways with either high predicted confidence or experimentally observed in human, rat or mouse were included in our analysis. The threshold for significant enrichment of a gene/protein pathway was set at a cutoff of $p < 0.05$ (corrected). Lists of all plasma membrane proteins were generated, and their abundance ratios were uploaded into IPA. To prioritize candidates for functional studies, we next analyzed relative expression differences (LogRatio) and corresponding *p*-values of plasma membrane proteins to identify top mechanistic networks [10] associated with the onset of memory deficits. Next, candidate proteins were narrowed by linking identified proteins to functions including Ca^{2+}-signaling, Ca^{2+} homeostasis, synaptic transmission and plasticity, neuronal excitability, and intrinsic neuronal plasticity.

2.5. Transcriptome profiling across BXDs

The BXD strains were derived by inbreeding the F2 progeny of C57Bl/6J and DBA/2J strains, generating a genetically diverse but inbred (therefore stable and reproducible) population of mice [11–14]. Whole-genome expression analysis of hippocampus mRNA [25] and contextual fear memory performance from 23 BXD strains [14] assessed previously were used to prioritize our top candidates. First, we compared differentially expressed transcript levels in the hippocampus relative to contextual memory rank across a genetically diverse population of inbred mice. Next, gene expression for Trpc genes (see Tables 1 and 2) was analyzed relative to contextual and cued memory rank in GeneNetwork (www.genenetwork.org) using established methods [25]. Spearman rank correlations for each Trpc gene were generated and adjusted for multiple comparisons using Bonferroni correction (95% confidence interval). Probes with highest and most consistent expression were selected and verified by BLAT (UCSC Genome Browser).

2.6. Slice preparation and electrophysiological recordings

Hippocampal slices were prepared as described previously [8]. Recording pipettes measured 2–3 MΩ and were filled with K-gluconate based intracellular solution [26]. The K-gluconate intracellular solution consisted of (in [mM]): 115 K-gluconate, 20 KCl, 10 sodium phosphocreatine (Na_2-Pcr), 10 HEPES, 2 MgATP, and 0.3 NaGTP [26]. KOH (1 M) was used to adjust the pH to 7.3–7.4. All reagents were purchased from Sigma–Aldrich (St. Louis, MO, USA), except KCl and HEPES (Fisher Scientific, Waltham, MA, USA). Whole-cell current-clamp recordings were made using a MultiClamp 700B (Molecular Devices, Downingtown, PA, USA) amplifier. Neurons resting between −60 mV and −75 mV were used for analysis. Neurons were maintained at a common membrane potential of −67 mV. Series resistance and capacitance were monitored and compensated throughout recordings; neurons with >40 MΩ series resistance were excluded from this study. Voltage responses were filtered at 5 kHz, digitized at 50 kHz and acquired *via* a Digidata 1440A interface (Molecular Devices, Downingtown, PA, USA). The post-burst afterhyperpolarization (AHP) was triggered using

Table 2
Trpc expression relative to performance on amygdala-dependent cued fear (Trait: 11010).

Gene	Probe set	Mean expression	Rho, Spearman rank	*p*-value (*N* = 23 BXD strains)
Trpc1	5409349	12.91	0.340	0.113
Trpc2	5330076	10.91	−0.155	0.484
Trpc3	5158157	10.52	−0.249	0.255
Trpc4	4719862	11.87	0.050	0.822
Trpc5	5280284	11.78	0.120	0.591
Trpc6	5329270	12.06	0.223	0.309
Trpc7	5138509	9.22	−0.071	0.930

25 brief (2 ms) somatic current injections (1 nA) at 50 Hz and monitored for no more than 20 min after gaining whole-cell access to minimize effects of AHP plasticity reported previously [27]. Membrane properties including the AHP were assessed as described [26]. Average APs in response to 100 pA were normalized to the baseline, which was recorded (10 min) prior to drug application, unless otherwise noted. The current intensity (100 pA) was selected given the average firing frequency matches spontaneously firing hippocampal neurons *in vivo* [28,29]. The TRPC3 antagonist HC-C3A was bath applied [30]. Fast excitatory neurotransmission was blocked with 20 μM 6-cyano-7-nitroquinoxaline-2,3-dione (CNQX) and 20 μM RS-3-(2 Carboxypiperazin-4-yl)-propyl-1-phosphonic acid (CPP) (Tocris). In addition, 50 μM picrotoxin (Sigma–Aldrich) was bath-applied in all experiments for the duration of the recording.

2.7. Adeno-associated viruses

The shRNA sequence targeting mouse TrpC3 mRNA (GAGGUUCAAUAUUUCACCUAGC; RefSeq NM_019510.2) was selected based on rational designs [31–39]. In addition, a non-targeting shRNA (GAGGAUCAAAUUGAUAGUAAACC), which showed no homology to any known genes (see below), was used as a control. All sequences were screened for sequence homology to other genes with NCBI-BLAST (www.ncbi.nlm.nih.gov/BLAST) and did not contain known immune response inducing motifs (GTCCTTCAA, CTGAATT, TGTGT, GTTGTGT) [40–43]. Oligos were custom synthesized (Life Technologies), resuspended using Duplex Buffer (Integrated DNA Technologies), and cloned into a "CreOff" adeno-associated virus (AAV) vector with a floxed cassette that comprises a U6 polymerase III promoter to drive shRNA expression and a CMV promoter to drive eGFP expression for identification of transduced neurons (see Supplementary Fig. 1). Constructs were cloned into pFB-AAV shuttle plasmid to allow for a baculovirus expression system-based AAV production [44]. AAV constructs were maintained and propagated with Stbl3 competent cells (Life Technologies) that harbors a mutation in recA gene specifically designed to reduce occurrence of unwanted recombination in cloned DNA. Strict attention was paid to the integrity of the vector inverted terminal repeats (ITRs) in plasmid preparations. All AAV plasmids were verified by diagnostic enzyme digestions. High titer ($1–2 \times 10^{13}$ GC/ml) AAVs with serotype 9 were commercially produced by Virovek (Hayward, CA) and selected based on transduction of neurons, but not microglia or oligodendrocytes in mouse brain [45,46]. Stereotaxic injections were performed as described directly below; Western blots were performed 4 weeks post injection to confirm efficacy of *Trpc3*-shRNA mediated knockdown *in vivo*.

2.8. Hippocampal injections of AAV

Mice were anesthetized using isoflurane gas (induction at 3.5%, maintenance at 1.5%) and positioned in a stereotaxic frame (Kopf Model 900). Analgesic was administered (Carprofen, 5–10 mg/kg). The skull was exposed and two holes made using a 21-guage needle (coordinates: anterior-posterior = −1.88 mm, medial-lateral = ±1.60 mm, and dorsal-ventral = −1.63 mm or −1.30 mm). A guide cannula was inserted and 1.0 μL of virus ($\sim 5.0 \times 10^{10}$ GC/μl of sterile saline) was delivered into each hemisphere through a 28 gauge microinjector attached to a Hamilton 5.0 μL syringe connected to an infusion pump (Harvard Apparatus) with an injection rate of 1.0 μL/min. The injector was left in place for an additional five minutes to allow the virus to diffuse. At the end of the procedure, the scalp was sutured and mice were allowed to recover over a heating pad. Analgesic was administered BID for 72 h after surgery (Carprofen, 5–10 mg/kg). The virus was allowed to incubate for at least four weeks before mice were used for subsequent behavioral testing, and sacrificed for collection of tissue for subsequent analyses.

2.9. Data acquisition and statistical analysis

Statistical analyses were performed using SPSS software (GraphPad Software, Inc., San Diego, CA, USA). Data were assessed for normality (Shapiro–Wilk's test) and equality of variance was assessed using Levene's test; analyses included paired and independent *t*-tests, one-way ANOVA, as well as repeated measures ANOVA with confidence level set at $p < 0.05$. All analyses were corrected appropriately for multiple comparisons and described in Results section. Unless otherwise stated, data values reported here are given as mean ± S.E.M. The order of samples run on the mass spectrometer (proteomics) for experimental groups, application of TRPC3 blockers, and mice in each condition were randomized. The experimenter was blind to the group allocation for all behavioral studies, and analysis of raw data was conducted blind to the experimental groups.

3. Results

Middle-aged mice (8–9 mo) were trained and tested on a standard contextual fear conditioning paradigm to distinguish those with early age-related memory impairment from those with intact memory per our prior report [8] (Fig. 1A; $n = 4$ mice/grp). We previously showed these differences in freezing during the contextual fear memory test did not result from differences in anxiolysis, expression of behavioral freezing, or sensory encoding, but were specific to hippocampus-dependent memory [8]. Unbiased monitoring combined with qualitative and quantitative analyses of the hippocampus proteome of impaired mice *versus* those with intact contextual fear memory was performed using label-free spectral counting (ms/ms) (Fig. 1B) [17,19,20]. Seven-hundred and one proteins annotated 'plasma membrane' using gene ontology [21] were identified in ≥3 of 4 mice per group using established criteria [19]; 57 plasma membrane ICRs were differentially expressed relative to memory status.

To prioritize candidates for functional studies, we utilized three main criteria: First, ICRs involved in one or more of the top three mechanistic networks (APP, 1.57×10^{-21}; PSEN1, 2.08×10^{-20}; and BDNF, 2.56×10^{-15}) associated with differences in contextual fear memory status [10,20] were identified using pathway analysis, which included CSF1R, GABBR2, LRP1B, NPR1, RYR2, SIRPA, and TRPC3. Next, candidate proteins with known functions in Ca^{2+} transport, Ca^{2+} homeostasis, and/or neuron excitability that could account for the reduced Ca^{2+}-dependent AHP in mice with intact contextual fear memory [47] were identified, narrowing candidates to GABBR2, LRP1B, RYR2, and TRPC3. Finally, gene expression in the hippocampus relative to contextual fear memory status was analyzed across 23 strains of a panel of genetically diverse inbred mice (BXD type) that were bred to model some of the diversity of human populations in traits including memory function [11,14]. Our analysis yielded two candidates meeting these criteria and whose transcript was significantly correlated with contextual fear memory status: GABBR2 ($r = -0.48$, $p < 0.05$) and TRPC3 ($r = -0.58$, $p < 0.001$). TRPC3 was selected based on the predominant expression in hippocampal pyramidal neurons [48] (Supplementary Figs. 2–4), in addition to the strong negative relationship between *Trpc3* transcript and contextual fear memory that mirrored TRPC3 protein expression changes identified by mass spectrometry (Fig. 1C and inset) and validated by Western blot ($t(1,4) = 3.02$, $p < 0.05$). Neither protein nor transcript for other *Trpc* genes was differentially expressed relative to contextual fear memory performance (Table 1). Moreover, analyses of *Trpc3*

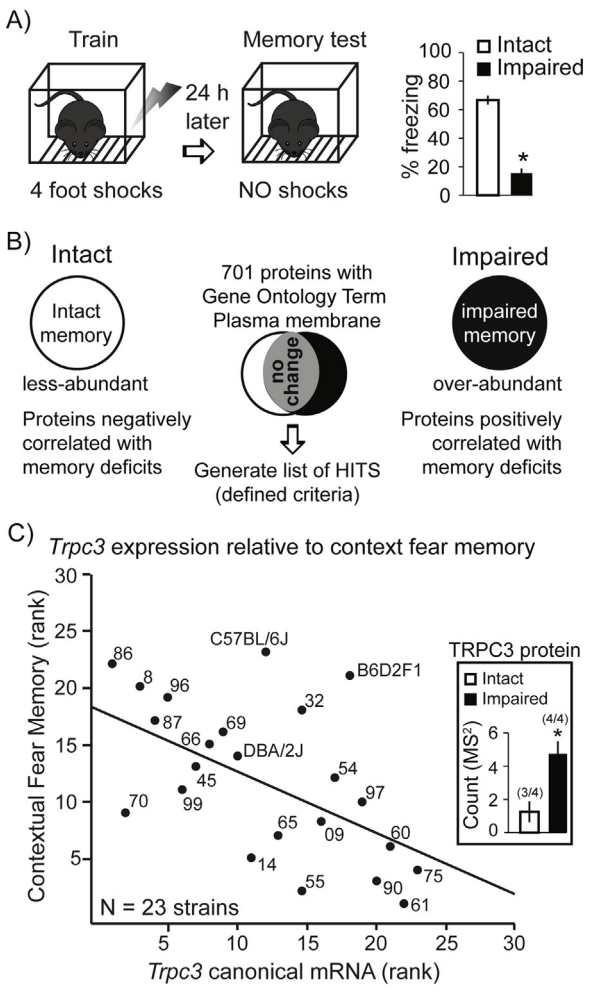

Fig. 1. Protein and transcript profiling identify TRPC3 as a putative negative regulator of contextual fear memory. (A) Contextual fear memory tests characterized mice as impaired relative to mice with intact memory. $N = 4$ mice/grp, one-tailed $t(1,6) = 11.3$, $^*p = 0.000015$. (B) Schematic of experimental design to identify ion channels and receptors differentially expressed relative to memory status *via* mass spectrometry [19]. (C) *Trpc3* transcript expression from hippocampus of 23 recombinant inbred strains (BXD type) revealed a negative relationship between expression of *Trpc3* and contextual fear memory abilities (Spearman rank correlation, $r = -0.58$, $p = 0.0038$), which corroborated increased TRPC3 protein in the hippocampus of impaired mice (inset, confirmed by Western blot, $^*p < 0.05$).

expression in the hippocampus transcriptome were not differentially expressed relative to cued fear memory, nor were other Trpc genes (Table 2). These data suggest TRPC3 acts as a negative regulator of hippocampus-dependent memory.

Previously, we reported hippocampal neurons of impaired mice have a larger Ca^{2+}-dependent afterhyperpolarization (AHP) than those of mice with intact contextual fear memory, thereby decreasing neuronal excitability and providing a mechanistic explanation for associated memory deficits [8,47]. Based on TRPC3 channel properties that include permeability to Ca^{2+} [49–51], we hypothesized TRPC3 channel activity contributes to the AHP. To test this hypothesis, electrophysiological experiments were conducted in hippocampal slices from mice aged P16-P21, as AHP properties from P16-P21 mice (mAHP -1.9 ± 1.0, sAHP $= -0.6 \pm 0.2$, $n = 9$ neurons/5 mice) are comparable to those measured in adult mice (2–3 mo; mAHP $= -2.0 \pm 0.6$, sAHP $= -0.5 \pm 0.1$, $n = 8$ neurons/3 mice). In support, the TRPC3 antagonist HC-C3A (1.5–3 μM; HydraBiosciences, MA) significantly reduced the AHP and increased excitability of hippocampal regular firing neurons (Fig. 2A–C). Intracellular block using anti-Trpc3 antibody [52] similarly increased hippocampal neuron excitability (Fig. 2D–F). When the anti-Trpc3 antibody was inactivated with heat, or sequestered with the antigen as a control (see Ab/anti, Fig. 2D–F), it had no effect compared to control on action potential firing. HC-C3A did not alter basic membrane properties including input resistance (R_{input}), current threshold ($I_{threshold}$), action potential (AP) threshold, AP height measured from spike threshold, or half-width (Table 3). HC-C3A at 3 μM also had no effect in slices from *Trpc3* knockout mice (Trpc3−/−), or after intracellular delivery of anti-Trpc3 antibody (Supplementary Fig. 5, $t(1,9) = -0.35$, $p = 0.74$), confirming selectivity of HC-C3A action at TRPC3 channels. Since recordings were performed in synaptic antagonists (CNQX, CPP and picrotoxin), the resulting changes in neuronal excitability with HC-C3A reflect an effect on intrinsic neuron properties. These data demonstrate a novel mechanism whereby TRPC3 negatively regulates neuronal excitability in the hippocampus. TRPC3 activity corresponds to a larger AHP and suppression of neuronal excitability, whereas blockade of TRPC3 channels enhances neuronal excitability by reducing the AHP.

Learning-related reductions in the AHP of hippocampal neurons have been proposed as a general mechanism underlying hippocampus-dependent memory [5]. We previously reported AHP reductions in hippocampal neurons after contextual fear conditioning, which may reflect a learning-related reduction in TRPC3. To test this hypothesis, we used Western blots to compare TRPC3 expression in the hippocampus of mice after fear conditioning and contextual fear memory test (Fig. 3A: FC memory index; $55.6 \pm 4.79\%$ freezing, $n = 9$ mice) to immediate shock deficit control mice that received shock but were not exposed to the training context for enough time on Day 1 to form an association between the context and shock [53] (Fig. 3A: ISD memory index; $8.85 \pm 3.06\%$ freezing, $n = 8$ mice), as well as naïve untrained controls ($n = 11$ mice). As hypothesized, TRPC3 expression was reduced by ~33% in the hippocampus of context fear conditioned mice relative to both ISD and naïve mice [Fig. 3B: one-way ANOVA $F(2,25) = 3.1$, $p = 0.032$ (one-tailed) with *post hoc* tests comparing FC relative to ISD ($p = 0.012$) and naïve cage controls ($p = 0.046$)]. These data demonstrate that contextual fear conditioning, but not conditioning where little to no learning occurs (ISD and naïve controls), corresponds to a reduction in TRPC3 channels in the hippocampus that likely contributes to plasticity necessary for successful performance on this hippocampus-dependent memory task. Together, these data suggest that removal or blockade of TRPC3 may effectively enhance contextual fear memory.

To initially test this hypothesis, Trpc3-/- mice generated on a Sv129 background [15] were trained on a standard delay fear conditioning paradigm. Sv129 wild-type (WT) littermates were used as controls. No differences in baseline activity, acquisition, or amygdala-dependent (cued fear) memory were observed (Fig. 4), suggesting *Trpc3* KO did not disrupt relevant sensory or motor function. However, Trpc3−/− mice performed superior to WT mice on hippocampus-dependent contextual fear memory test (6 min) (Fig. 4B). These data support our hypothesis that TRPC3 modulates contextual fear memory, as TRPC3 deletion distinctively enhances hippocampus-dependent contextual fear memory. Because TRPC3 is ubiquitously deleted in Trpc3−/− mice [15], it is possible that deletion of TRPC3 during development and/or in other brain regions contributes to enhanced contextual fear memory in Trpc3−/− mice. Therefore, we used adeno-associated virus (AAV9) to deliver either *Trpc3* or non-targeting shRNA (Supplementary Fig. 1) to the hippocampus of C57Bl/6 mice and directly test the hypothesis that reduction in TRPC3 channels in the hippocampus enhance contextual fear memory. The C57Bl/6 mouse was chosen for subsequent validation studies for a variety of reasons, including the fact that this model is readily available, widely studied, and a moderate learner of contextual fear memory and other

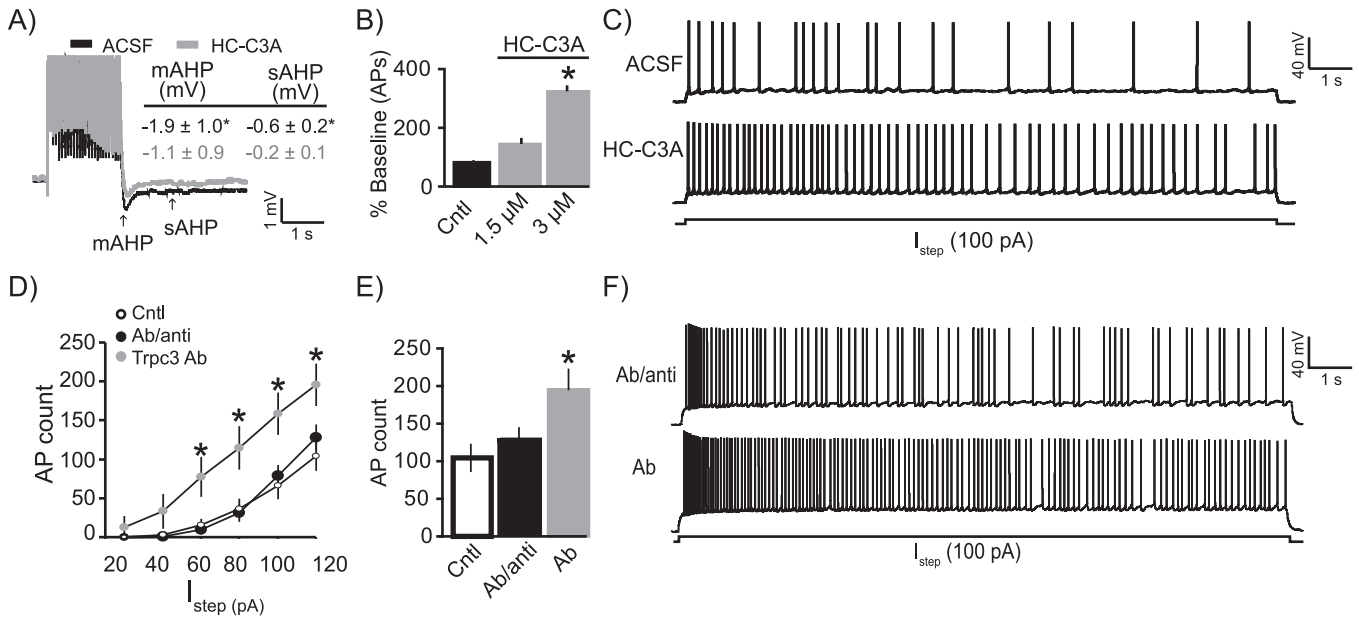

Fig. 2. TRPC3 channels modulate hippocampal neuron excitability phenotype associated with contextual memory. (A) The selective TRPC3 blocker HC-C3A significantly reduced both the medium (mAHP) and slow (sAHP) components of the post-burst AHP triggered by 25 brief (2 ms) current steps (1 nA) at a frequency of 50 Hz in CD1 mice, $n = 14$ neurons, paired $t(13) = 2.63$, $p = 0.021$. (B) HC-C3A dose-dependently increased firing compared to control ($n = 9$ neurons/9 slices/5 mice); one-way ANOVA $F(2,22) = 5.61$, $p = 0.012$. Low (1.5 μM HC-C3A, $n = 5$ neurons/5 slices/3 mice) and high (3 μM HC-C3A, $n = 9$ neurons/9 slices/7 mice). (C) Representative traces illustrate HC-C3A increased firing (100 pA, 15 s). (D) Intracellular blockade of TRPC3 with Trpc3-antibody [52] significantly increased the action potential frequency across a range of depolarizing current steps (Trpc3 Ab, $n = 8$ neurons/8 slices/4 mice) relative to standard controls (ACSF, $n = 21$ neurons/21 slices/13 mice) and heat-inactivated Trpc3 antibody controls (Ab/anti, $n = 9$ neurons/9 slices/4 mice), repeated-measures ANOVA $F(2,35) = 6.85$, $p = .003$; *post hoc* LSD test, $^*p < 0.05$). (E) Mean action potential count in response to a 100 pA current step, *post hoc* LSD test ($^*p < 0.02$). (F) Intracellular blockade of Trpc3 increases firing. Experiments conducted in ionotropic inhibitory and excitatory receptor blockers; changes in firing reflect intrinsic properties.

Table 3
Intrinsic membrane properties following HC-C3A blockade of TRPC3 channels.

	R_{input}	$I_{threshold}$	AP threshold	AP height	Half-width
Synaptic blockers	112.0 ± 24.5	1245 ± 113	−52.1 ± 0.8	91.8 ± 2.6	0.80 ± 0.03
HC-C3A	125.9 ± 36.9	1219 ± 107	−52.2 ± 1.5	87.7 ± 3.5	0.84 ± 0.04

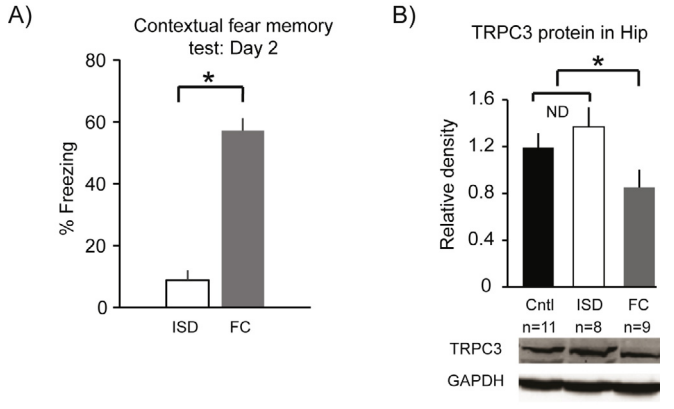

Fig. 3. TRPC3 is downregulated in the hippocampus following contextual fear conditioning (FC). (A) Plot showing mice trained on immediate shock deficit (ISD) paradigm exhibit a deficit in shock:context associative memory compared to mice trained on standard FC (memory index; 55.6 ± 4.79% freezing, $n = 9$ mice) as evidenced by a significant decrease in the average time spent freezing over 10-min test of contextual fear memory on Day 2 in ISD mice (8.85% ± 3.06% freezing, $n = 8$ mice); $t(1,15) = -9.31$, $p < 0.001$. (B) Plot showing TRPC3 protein is decreased in the hippocampus of adult C57Bl/6J mice after contextual fear conditioning compared to naive cage controls (Cntl; $n = 11$ mice) and ISD controls [One-way ANOVA $F(2,25) = 3.1$, $p = 0.032$ with *post hoc* tests comparing FC relative to ISD ($p = 0.012$) and naïve cage controls ($p = 0.046$)]. Representative western blot images are shown below the graph.

hippocampus dependent tasks, thus ensuring that either enhancement or impairment following TRPC3 manipulation could be observed – limiting bias from potential floor or ceiling effects [54].

Trpc3 shRNA reliably decreased protein expression in the hippocampus by 25% following 4 week incubation *in vivo* ($t(1,4) = -3.49$, $p = 0.03$; $n = 3$ mice/grp). Next, we evaluated contextual fear memory using a standard delay conditioning paradigm. Virally-mediated knockdown of TRPC3 in the hippocampus had

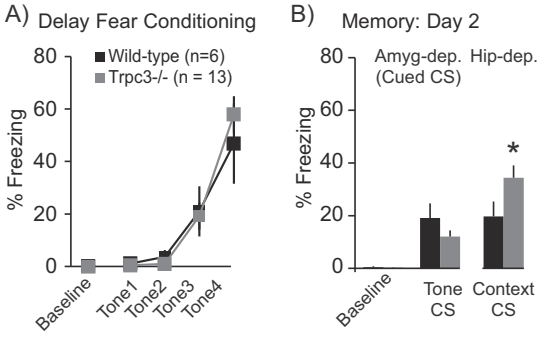

Fig. 4. Trpc3−/− mice exhibited enhanced contextual fear memory compared to WT littermate controls. (A) In Trpc3−/− mice ($n = 13$), baseline freezing and tone CS freezing during auditory delay fear conditioning were similar to age-matched Sv129 wild-type mice ($n = 6$). (B) Test of amygdala dependent memory on day 2 revealed no differences in baseline activity ($t(1,17) = 0.5$, $p = 0.64$) or retention of the tone CS memory (average of tone CS 1–4, $(1,17) = 1.4$, $p = 0.18$), but a specific and significant enhancement of hippocampus-dependent contextual fear memory in Trpc3−/− (gray) relative to WT mice (black), $t(1,17) = 1.9$, $^*p = 0.04$, one-tailed.

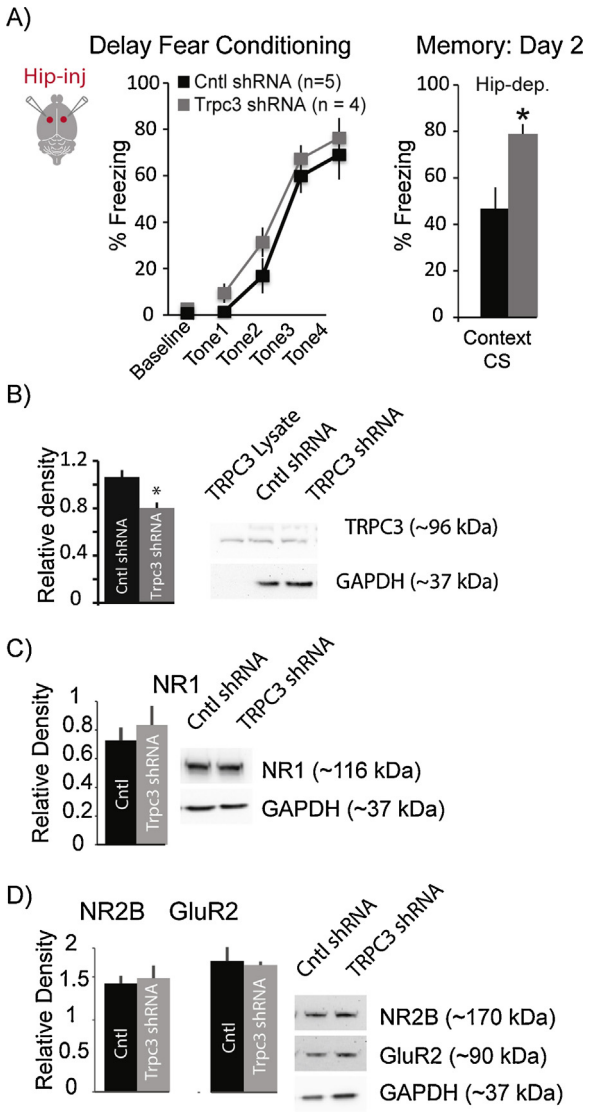

Fig. 5. Targeted knockdown of TRPC3 in the hippocampus enhances contextual fear conditioning, independently of 'classical' mediators of synaptic plasticity. (A) In mice that received intra-hippocampal AAV9-Trpc3 shRNA ($n=4$) or non-targeting sequence ($n=5$) 4 weeks prior ($\sim 5.0 \times 10^{10}$ GC/μl), measures of baseline freezing and tone CS freezing during auditory delay fear conditioning were comparable. Right plot shows hippocampus-dependent contextual fear memory was enhanced in mice that received AAV9-Trpc3 shRNA compared to non-targeting sequence, one-tailed $t(1,7)=2.91$, $^*p=0.011$. (B) Western blots confirmed a ~25% decrease in Trpc3-shRNA in AAV vectors *in vivo* relative to GAPDH loading control, ($t(1,4)$ −3.49, $p=0.03$; $n=3$ mice/grp). AAVs were produced commercially by Virovek (Hayward, CA). Representative images of TRPC3 and GAPDH expression in hippocampus samples from mice that received either shRNA for *Trpc3* or a non-targeting sequence. TRPC3 lysate confirmed specificity of antibody for TRPC3 at the predicted molecular weight. (C) Western blots examining 'classical' mediators of synaptic plasticity such as NR1, (D) NR2B, and GluR2 show that protein expression of these subunits was not significantly altered by *Trpc3* shRNA treatment, $n=3$ mice/grp.

no effect on baseline fear measures, sensitivity to shock as measured by average post-shock activity burst ($t(1,7)=0.62$, $p=0.46$), or acquisition of delay fear conditioning paradigm relative to non-targeting control (Fig. 5A). Yet, targeted knockdown of TRPC3 in the hippocampus significantly enhanced contextual fear memory (Fig. 5A, Day2). This result is consistent with the superior contextual fear memory observed in Trpc3−/− relative to WT mice. Interestingly, TRPC3 mediated enhancement of contextual fear memory was independent of changes in the expression of several 'classical' receptors shown to mediate synaptic plasticity [55], a leading candidate for information storage [($NMDA_R$ subunit (NR2B; $t(1,4)$ 0.35, $p=0.75$), $NMDA_R$ subunit (NR1; $t(1,4)$ 0.66, $p=0.55$), and $AMPA_R$ subunit (GluR2; $t(1,4)$ 0.28, $p=0.78$); Fig. 5C and D)]. Taken together, our results demonstrate that TRPC3 is a key regulator of hippocampal neuronal excitability and hippocampus-dependent memory.

4. Discussion

De novo protein synthesis is critical for the establishment of long-term memories, yet the identification of the exact molecular mediators of memory have remained elusive. Pioneering studies have utilized information such as localization [56] and known function [57,58] to develop hypotheses regarding putative candidates mediating memory formation including NMDA receptor subunit NR2B [57], $GABA_A$ receptor subunit α5 [56], and the neurokinin3 receptor [59], and others [60–62] that have been elegantly validated using both pharmacological and genetic approaches. Despite multiple advances in the identification of molecules that have a role in memory formation, there remains a lack of neurocognitive enhancers that have effectively translated into therapeutic targets for the treatment of both normal and disease-related cognitive decline [63]. Thus, there is still considerable need to elucidate additional mechanisms underlying memory, identify key mediators, and generate novel targets for future drug development. To this end, we developed a novel approach which allowed us to exploit differences in memory function in mouse models and discover novel candidates, which ultimately resulted in the identification and subsequent validation of TRPC3 as a novel mediator of hippocampal neuronal excitability and contextual fear memory.

The classification of animals as either cognitively impaired or unimpaired allowed us to exploit the phenotypic heterogeneity of a population in order to identify mechanisms specifically implicated in the regulation of memory [8,64–67]. Previously, it has been shown that animals from various species exhibiting impaired memory also exhibit decreased neuron excitability *via* enhancement of the Ca^{2+}-dependent post-burst AHP [8,47]. This reduced excitability is thought to prevent neurons from becoming part of the neural network that is recruited during information storage, therefore providing a mechanistic explanation for memory deficits [5]. As plasma membrane ICRs are known to be key regulators of excitability [68], we performed an in-depth analysis of the hippocampus membrane proteome, which allowed us to monitor hundreds of non-redundant plasma membrane proteins simultaneously. This allowed for both the identification of proteins not previously associated with this complex process and the generation of novel hypotheses regarding molecular memory mechanisms. Furthermore, utilizing a proteomics approach allowed us to monitor those molecules whose changes in expression were most likely to result in functional changes at the cellular level [69]. Thus, by using an in-depth and targeted proteomics approach on a behaviorally characterized population, we optimized our ability to detect proteins whose changes in expression were playing a novel functional role in the regulation of memory function. In addition to the evidence provided here for the functional importance of TRPC3, our second putative candidate, GABBR2, was recently shown to have a novel role in regulating long-term spatial memory [70], providing independent secondary evidence for the validity of this approach for the identification of molecular mediators of memory function.

Collectively, our data suggests overexpression of TRPC3 observed in the hippocampus of aging mice may play a role in mediating the enhanced AHP, decreased neuronal excitability, and early-onset memory deficits that we and others reported previously in both aging and AD models [5,8,47,71,72]. In support, it was recently demonstrated that caloric restriction of aging mice sufficient to improve memory function corresponds to a decrease in

hippocampal *Trpc3* expression [73] and prevention of aging-related changes in the post-burst AHP [74].

Given that blockade or downregulation of TRPC3 potently reduces the AHP and enhances contextual fear memory of adult *unimpaired* mice, therapeutics that either reduce the expression or impair function of TRPC3 channels may serve as a new line of neurocognitive enhancers. Overall, we demonstrate a novel workflow for drug discovery that combines targeted proteomics, population-based transcriptome profiling, knowledge-based bioinformatics, behavioral assays, and viral-mediated gene knockdown in order to progress from a list of hundreds of non-redundant proteins to the identification and functional validation of a novel molecular mediator of contextual fear memory, the ion channel TRPC3.

Author contributions

C.C.K. conceived of the experiments and designed the experiments. S.M.N., L.A.W., K.A.H. and C.C.K. performed the experiments. S.M.N., L.A.W., K.A.H., B.H., K.M.O. and C.C.K. analyzed the data. J.A.C., J.A., L.B., C.S.C., A.K.T., A.S.G. and C.C.K. contributed reagents/materials/analysis tools. C.C.K. and S.M.N. wrote the manuscript. All authors reviewed and contributed intellectually to the final manuscript.

Acknowledgments

This work was supported in part by the Intramural Research Program of the National Institutes of Health (ZO1-ES-101684 to L.B.). S.M.N. and K.A.H. were supported by the University of Tennessee Health Science Center, Neuroscience Institute. B.H. was supported by the Biotechnology Training Grant (T32-HL-094273) and generous support from the Robert and Patricia Kern Foundation. A.S.G. was supported by P01-HL-082798 (PI: Greene). C.S.C. was supported by R01-NS-069777 and DoD W81XWH-13-1-0243 (PI: Chan). C.C.K. and L.A.W. were supported by K99/R00-AG-039511 (PI: Kaczorowski).

The authors wish to thank Dr. Kate Noon for exceptional technical support on the design and analysis of the hippocampus membrane proteome and Dr. Robert Williams for assistance on transcriptome analysis in BXDs. We also thank Dr. Shannon Moore for her thoughtful comments on the manuscript, and Caroline Cook for her work on the illustrations.

Appendix A. Supplementary data

Supplementary data associated with this article can be found, in the online version, at http://dx.doi.org/10.1016/j.bbr.2014.12.018.

References

[1] Davis HP, Squire LR. Protein synthesis and memory: a review. Psychol Bull 1984;96:518–59.
[2] McGaugh JL. Memory—a century of consolidation. Science 2000;287:248–51.
[3] Hernandez PJ, Abel T. The role of protein synthesis in memory consolidation: progress amid decades of debate. Neurobiol Learn Mem 2008;89:293–311.
[4] Jarome TJ, Helmstetter FJ. Protein degradation and protein synthesis in long-term memory formation. Front Mol Neurosci 2014;7:61.
[5] Oh MM, Oliveira FA, Disterhoft JF. Learning and aging related changes in intrinsic neuronal excitability. Front Aging Neurosci 2010;2:2.
[6] Zhang W, Linden DJ. The other side of the engram: experience-driven changes in neuronal intrinsic excitability. Nat Rev Neurosci 2003;4:885–900.
[7] Giese KP, Peters M, Vernon J. Modulation of excitability as a learning and memory mechanism: a molecular genetic perspective. Physiol Behav 2001;73:803–10.
[8] Kaczorowski CC, Disterhoft JF. Memory deficits are associated with impaired ability to modulate neuronal excitability in middle-aged mice. Learn Mem 2009;16:362–6.
[9] Bliss TV, Collingridge GL. A synaptic model of memory: long-term potentiation in the hippocampus. Nature 1993;361:31–9.
[10] Kramer A, Green J, Pollard Jr J, Tugendreich S. Causal analysis approaches in Ingenuity Pathway Analysis. Bioinformatics 2014;30:523–30.
[11] Peirce JL, Lu L, Gu J, Silver LM, Williams RW. A new set of BXD recombinant inbred lines from advanced intercross populations in mice. BMC Genet 2004;5:7.
[12] Taylor BA, Wnek C, Kotlus BS, Roemer N, MacTaggart T, Phillips SJ. Genotyping new BXD recombinant inbred mouse strains and comparison of BXD and consensus maps. Mamm Genome 1999;10:335–48.
[13] Williams RW, Gu J, Qi S, Lu L. The genetic structure of recombinant inbred mice: high-resolution consensus maps for complex trait analysis. Genome Biol 2001;2. Research0046.
[14] Brigman JL, Mathur P, Lu L, Williams RW, Holmes A. Genetic relationship between anxiety-related and fear-related behaviors in BXD recombinant inbred mice. Behav Pharmacol 2009;20:204–9.
[15] Hartmann J, Dragicevic E, Adelsberger H, Henning HA, Sumser M, Abramowitz J, et al. TRPC3 channels are required for synaptic transmission and motor coordination. Neuron 2008;59:392–8.
[16] Chen C, Kim JJ, Thompson RF, Tonegawa S. Hippocampal lesions impair contextual fear conditioning in two strains of mice. Behav Neurosci 1996;110:1177–80.
[17] Wisniewski JR, Zougman A, Nagaraj N, Mann M. Universal sample preparation method for proteome analysis. Nat Methods 2009;6:359–62.
[18] Halligan BD, Geiger JF, Vallejos AK, Greene AS, Twigger SN. Low cost, scalable proteomics data analysis using Amazon's cloud computing services and open source search algorithms. J Proteome Res 2009;8:3148–53.
[19] Halligan BD, Greene AS. Visualize: a free and open source multifunction tool for proteomics data analysis. Proteomics 2011;11:1058–63.
[20] Kaczorowski CC, Stodola TJ, Hoffmann BR, Prisco AR, Liu PY, Didier DN, et al. Targeting the endothelial progenitor cell surface proteome to identify novel mechanisms that mediate angiogenic efficacy in a rodent model of vascular disease. Physiol Genomics 2013;45:999–1011.
[21] Ashburner M, Ball CA, Blake JA, Botstein D, Butler H, Cherry JM, et al. Gene ontology: tool for the unification of biology. The Gene Ontology Consortium. Nat Genet 2000;25:25–9.
[22] Shirakawa H, Sakimoto S, Nakao K, Sugishita A, Konno M, Iida S, et al. Transient receptor potential canonical 3 (TRPC3) mediates thrombin-induced astrocyte activation and upregulates its own expression in cortical astrocytes. J Neurosci 2010;30:13116–29.
[23] Murata Y, Constantine-Paton M. Postsynaptic density scaffold SAP102 regulates cortical synapse development through EphB and PAK signaling pathway. J Neurosci 2013;33:5040–52.
[24] Romero-Calvo I, Ocon B, Martinez-Moya P, Suarez MD, Zarzuelo A, Martinez-Augustin O, et al. Reversible Ponceau staining as a loading control alternative to actin in Western blots. Anal Biochem 2010;401:318–20.
[25] Mozhui K, Wang X, Chen J, Mulligan MK, Li Z, Ingles J, Chen X, Lu L, Williams RW. Genetic regulation of Nrnx1 expression: an integrative cross-species analysis of schizophrenia candidate genes. Transl Psychiatry 2011;1e38:1–11.
[26] Kaczorowski CC, Disterhoft J, Spruston N. Stability and plasticity of intrinsic membrane properties in hippocampal CA1 pyramidal neurons: effects of internal anions. J Physiol 2007;578:799–818.
[27] Kaczorowski CC. Bidirectional pattern-specific plasticity of the slow after hyperpolarization in rats: role for high-voltage activated Ca^{2+} channels and I h. Eur J Neurosci 2011;34:1756–65.
[28] Sharp PE, Green C. Spatial correlates of firing patterns of single cells in the subiculum of the freely moving rat. J Neurosci 1994;14:2339–56.
[29] Deadwyler SA, Hampson RE. Differential but complementary mnemonic functions of the hippocampus and subiculum. Neuron 2004;42:465–76.
[30] Chong JA, Lacey V, Guiliano M, Fanger CM, Moran MM, del Camino D. Novel TRPC3 and TRPC6 antagonists identified. Chicago, IL: Society for Neuroscience; 2008.
[31] Ui-Tei K, Naito Y, Takahashi F, Haraguchi T, Ohki-Hamazaki H, Juni A, et al. Guidelines for the selection of highly effective siRNA sequences for mammalian and chick RNA interference. Nucleic Acids Res 2004;32:936–48.
[32] Amarzguioui M, Prydz H. An algorithm for selection of functional siRNA sequences. Biochem Biophys Res Commun 2004;316:1050–8.
[33] Hsieh AC, Bo R, Manola J, Vazquez F, Bare O, Khvorova A, et al. A library of siRNA duplexes targeting the phosphoinositide 3-kinase pathway: determinants of gene silencing for use in cell-based screens. Nucleic Acids Res 2004;32:893–901.
[34] Takasaki S, Kotani S, Konagaya A. An effective method for selecting siRNA target sequences in mammalian cells. Cell Cycle 2004;3:790–5.
[35] Huesken D, Lange J, Mickanin C, Weiler J, Asselbergs F, Warner J, et al. Design of a genome-wide siRNA library using an artificial neural network. Nat Biotechnol 2005;23:995–1001.
[36] Ichihara M, Murakumo Y, Masuda A, Matsuura T, Asai N, Jijiwa M, et al. Thermodynamic instability of siRNA duplex is a prerequisite for dependable prediction of siRNA activities. Nucleic Acids Res 2007;35:e123.
[37] Reynolds A, Leake D, Boese Q, Scaringe S, Marshall WS, Khvorova A. Rational siRNA design for RNA interference. Nat Biotechnol 2004;22:326–30.
[38] Katoh T, Suzuki T. Specific residues at every third position of siRNA shape its efficient RNAi activity. Nucleic Acids Res 2007;35:e27.
[39] Vert JP, Foveau N, Lajaunie C, Vandenbrouck Y. An accurate and interpretable model for siRNA efficacy prediction. BMC Bioinform 2006;7:520.
[40] Judge AD, Sood V, Shaw JR, Fang D, McClintock K, MacLachlan I. Sequence-dependent stimulation of the mammalian innate immune response by synthetic siRNA. Nat Biotechnol 2005;23:457–62.

[41] Robbins M, Judge A. MacLachlan I. siRNA and innate immunity. Oligonucleotides 2009;19:89–102.
[42] Hornung V, Guenthner-Biller M, Bourquin C, Ablasser A, Schlee M, Uematsu S, et al. Sequence-specific potent induction of IFN-alpha by short interfering RNA in plasmacytoid dendritic cells through TLR7. Nat Med 2005;11:263–70.
[43] Lan T, Putta MR, Wang D, Dai M, Yu D, Kandimalla ER, et al. Synthetic oligoribonucleotides-containing secondary structures act as agonists of Toll-like receptors 7 and 8. Biochem Biophys Res Commun 2009;386:443–8.
[44] Chen H. Intron splicing-mediated expression of AAV Rep and Cap genes and production of AAV vectors in insect cells. Mol Ther 2008;16:924–30.
[45] Dufour BD, Smith CA, Clark RL, Walker TR, McBride JL. Intrajugular vein delivery of AAV9-RNAi prevents neuropathological changes and weight loss in Huntington's disease mice. Mol Ther 2014;22:797–810.
[46] Gray SJ, Matagne V, Bachaboina L, Yadav S, Ojeda SR, Samulski RJ. Preclinical differences of intravascular AAV9 delivery to neurons and glia: a comparative study of adult mice and nonhuman primates. Mol Ther 2011;19:1058–69.
[47] Kaczorowski CC, Sametsky E, Shah S, Vassar R, Disterhoft JF. Mechanisms underlying basal and learning-related intrinsic excitability in a mouse model of Alzheimer's disease. Neurobiol Aging 2011;32:1452–65.
[48] Chung YH, Sun Ahn H, Kim D, Hoon Shin D, Su Kim S, Yong Kim K, et al. Immunohistochemical study on the distribution of TRPC channels in the rat hippocampus. Brain Res 2006;1085:132–7.
[49] Clapham DE. TRP channels as cellular sensors. Nature 2003;426:517–24.
[50] Boulay G, Zhu X, Peyton M, Jiang M, Hurst R, Stefani E, et al. Cloning and expression of a novel mammalian homolog of *Drosophila* transient receptor potential (Trp) involved in calcium entry secondary to activation of receptors coupled by the Gq class of G protein. J Biol Chem 1997;272:29672–80.
[51] Zitt C, Obukhov AG, Strubing C, Zobel A, Kalkbrenner F, Luckhoff A, et al. Expression of TRPC3 in Chinese hamster ovary cells results in calcium-activated cation currents not related to store depletion. J Cell Biol 1997;138:1333–41.
[52] Zhou FW, Matta SG, Zhou FM. Constitutively active TRPC3 channels regulate basal ganglia output neurons. J Neurosci 2008;28:473–82.
[53] Wiltgen BJ, Sanders MJ, Anagnostaras SG, Sage JR, Fanselow MS. Context fear learning in the absence of the hippocampus. J Neurosci 2006;26:5484–91.
[54] Crawley JN, Belknap JK, Collins A, Crabbe JC, Frankel W, Henderson N, et al. Behavioral phenotypes of inbred mouse strains: implications and recommendations for molecular studies. Psychopharmacology 1997;132:107–24.
[55] Lynch MA. Long-term potentiation and memory. Physiol Rev 2004;84:87–136.
[56] Collinson N, Kuenzi FM, Jarolimek W, Maubach KA, Cothliff R, Sur C, et al. Enhanced learning and memory and altered GABAergic synaptic transmission in mice lacking the alpha 5 subunit of the GABAA receptor. J Neurosci 2002;22:5572–80.
[57] Tang YP, Shimizu E, Dube GR, Rampon C, Kerchner GA, Zhuo M, et al. Genetic enhancement of learning and memory in mice. Nature 1999;401:63–9.
[58] Nolan MF, Malleret G, Dudman JT, Buhl DL, Santoro B, Gibbs E, et al. A behavioral role for dendritic integration: HCN1 channels constrain spatial memory and plasticity at inputs to distal dendrites of CA1 pyramidal neurons. Cell 2004;119:719–32.
[59] de Souza Silva MA, Lenz B, Rotter A, Biermann T, Peters O, Ramirez A, et al. Neurokinin3 receptor as a target to predict and improve learning and memory in the aged organism. Proc Natl Acad Sci USA 2013;110:15097–102.
[60] Frank DA, Greenberg ME. CREB: a mediator of long-term memory from mollusks to mammals. Cell 1994;79:5–8.
[61] Murase S, Schuman EM. The role of cell adhesion molecules in synaptic plasticity and memory. Curr Opin Cell Biol 1999;11:549–53.
[62] Hawkins RD, Kandel ER, Bailey CH. Molecular mechanisms of memory storage in Aplysia. Biol Bull 2006;210:174–91.
[63] Borbely E, Scheich B, Helyes Z. Neuropeptides in learning and memory. Neuropeptides 2013;47:439–50.
[64] Thompson LT, Moyer Jr JR, Disterhoft JF. Trace eyeblink conditioning in rabbits demonstrates heterogeneity of learning ability both between and within age groups. Neurobiol Aging 1996;17:619–29.
[65] Gallagher M, Rapp PR. The use of animal models to study the effects of aging on cognition. Annu Rev Psychol 1997;48:339–70.
[66] Gallagher M, Bizon JL, Hoyt EC, Helm KA, Lund PK. Effects of aging on the hippocampal formation in a naturally occurring animal model of mild cognitive impairment. Exp Gerontol 2003;38:71–7.
[67] VanGuilder HD, Farley JA, Yan H, Van Kirk CA, Mitschelen M, Sonntag WE, et al. Hippocampal dysregulation of synaptic plasticity-associated proteins with age-related cognitive decline. Neurobiol Dis 2011;43:201–12.
[68] Schulz DJ. Plasticity and stability in neuronal output via changes in intrinsic excitability: it's what's inside that counts. J Exp Biol 2006;209:4821–7.
[69] Jensen ON. Interpreting the protein language using proteomics. Nat Rev 2006;7:391–403.
[70] Terunuma M, Revilla-Sanchez R, Quadros IM, Deng Q, Deeb TZ, Lumb M, et al. Postsynaptic GABAB receptor activity regulates excitatory neuronal architecture and spatial memory. J Neurosci 2014;34:804–16.
[71] Campbell LW, Hao SY, Thibault O, Blalock EM, Landfield PW. Aging changes in voltage-gated calcium currents in hippocampal CA1 neurons. J Neurosci 1996;16:6286–95.
[72] Tombaugh GC, Rowe WB, Rose GM. The slow after hyperpolarization in hippocampal CA1 neurons covaries with spatial learning ability in aged Fisher 344 rats. J Neurosci 2005;25:2609–16.
[73] Schafer M, Dolgalev I, Heguy A, Ginsberg SD. Calorie restriction reverses age-dependent gene expression and induces neuroprotective transcriptional signatures in the hippocampal CA1 region. Washington, DC: Society for Neuroscience; 2014.
[74] Hemond P, Jaffe DB. Caloric restriction prevents aging-associated changes in spike-mediated Ca^{2+} accumulation and the slow after hyperpolarization in hippocampal CA1 pyramidal neurons. Neuroscience 2005;135:413–20.

Supplementary Methods

Immunohistochemistry

Mice were anesthetized with avertin and perfused with PBS followed by 4% paraformaldehyde in PBS. Brains were removed and post-fixed hemi-brains (4% PFA at 4°C) from mice were embedded in agarose and 50 μM coronal sections were cut on a vibrating microtome (Leica VT1000S). Sections were washed with PBS and incubated in sodium borohydride (1% w/v) for 30 minutes. Sections were washed with PBS, incubated in 5% normal donkey serum for 2 hours at room temperature, and labelled with rabbit anti-Trpc3 primary antibodies (Novus Biologicals, NB-110-74935). Sections for dual-labelling with anti-Trpc3 and goat anti-GFAP (Santa Cruz, SC6170) also included 0.05% Tween-20. Both primary antibodies were applied at 1:300. Slices were incubated at 4°C overnight and then washed with PBS. Secondary antibodies donkey anti-rabbit 568 (Invitrogen, A10042) and donkey anti-goat 488 (Invitrogen, A11055) were applied at 1:500 and incubated overnight. Slices were then washed with PBS and mounted with polyvinyl alcohol mounting medium with DABCO antifade (Fluka). Confocal imaging was performed as described previously[39]. Images were acquired with ZEN software (Zeiss).

Supplementary Figures

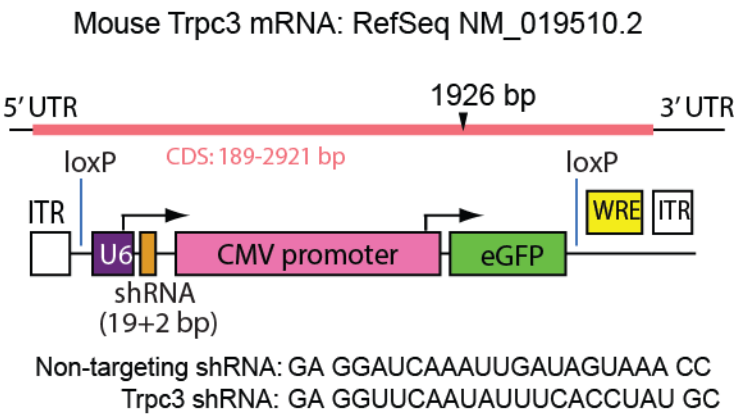

Supplementary Figure 1: Schematic of AAV-*Trpc3*-shRNA construction for *in vivo* knockdown in hippocampus. Constructs were packaged into a recombinant adeno-associated virus (AAV9 serotype) vector system that consisted of two transcription units, one encoding shRNA under the control of the U6 promoter and another encoding EGFP under the control of the cytomegalovirus (CMV) promoter. In this vector, the U6-shRNA cassette upstream of the CMV-EGFP expression cassette was flanked by two LoxP sequences. The first LoxP sequence was placed in an upstream region of the U6 promoter partially dispensable for its activity. The second is located downstream of the CMV-EGFP cassette. Expression of EGFP was used as an index of effective transduction of the AAV vector and detection of deposition site following stereotaxic injection. AAVs were produced commercially by Virovek (Hayward, CA) (titer; ~5.0 x 10^{10} GC/µl).

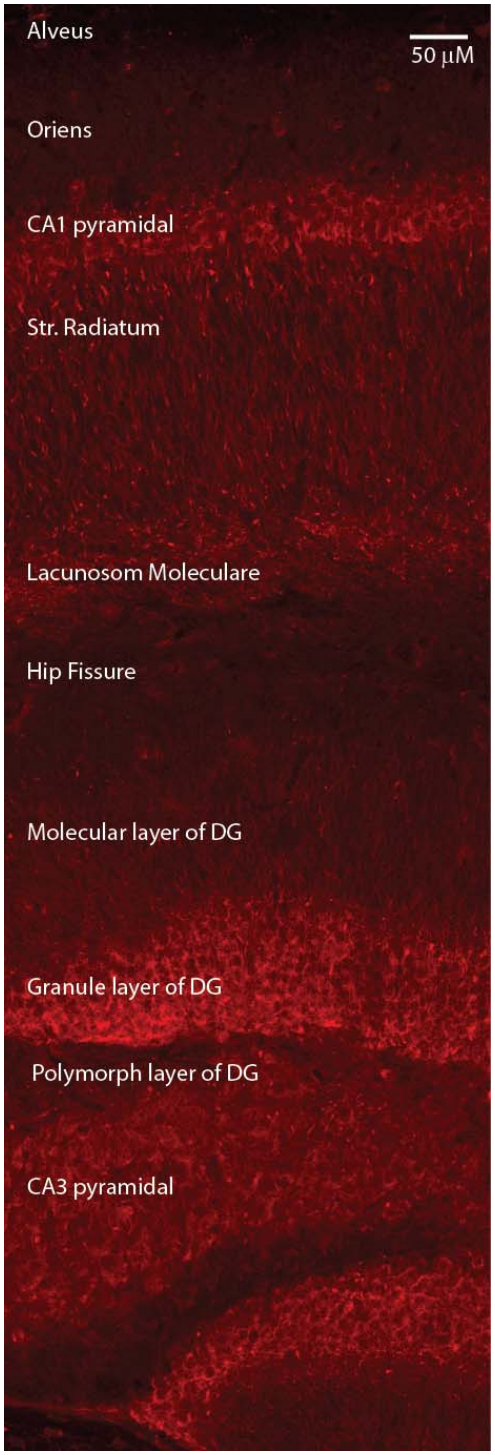
Alveus
50 μM
Oriens
CA1 pyramidal
Str. Radiatum
Lacunosom Moleculare
Hip Fissure
Molecular layer of DG
Granule layer of DG
Polymorph layer of DG
CA3 pyramidal

Supplementary Figure 2: TRPC3 is widely expressed in cell bodies located in pyramidal layer of the hippocampus proper. Representative image of TRPC3 expression in the hippocampus of a wild-type mouse following immunohistochemical labelling and confocal imaging demonstrate an expression pattern that is consistent with prior report[46]. Specifically, we observe TRPC3 in the CA1 and CA3 pyramidal layers, as well as the granule layer of dentate gyrus. TRPC3 expression is also high in dendritic processes projecting from the CA1 pyramidal layer into the stratum radiatum.

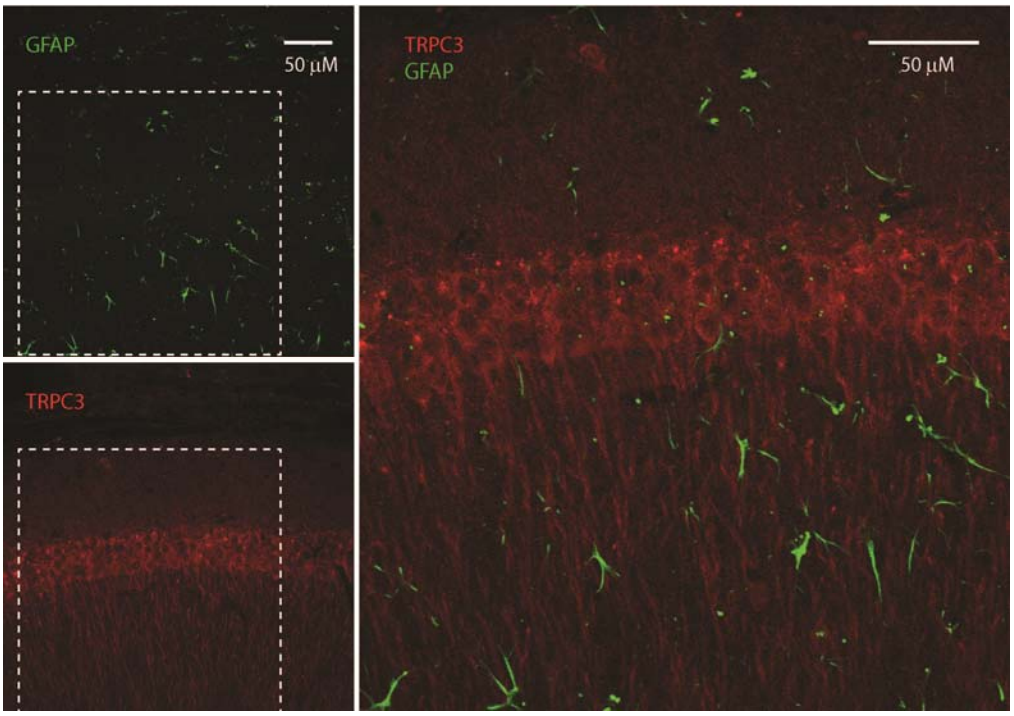

Supplementary Figure 3: TRPC3 is expressed in neurons, but not astrocytes, in the hippocampus of wild-type mice. Immunohistochemistry labeling and imaging of the astrocyte marker GFAP (top left, green) and TRPC3 (bottom left, red) in the CA1 region of the hippocampus suggest that astrocytes in wild-type mice do not express Trpc3. Representative overlay of the red and green channels (right) shows no colocalization of Trpc3 and GFAP (absence of yellow), indicating TRPC3 is not expressed in astrocytes within the hippocampus in wild-type mice.

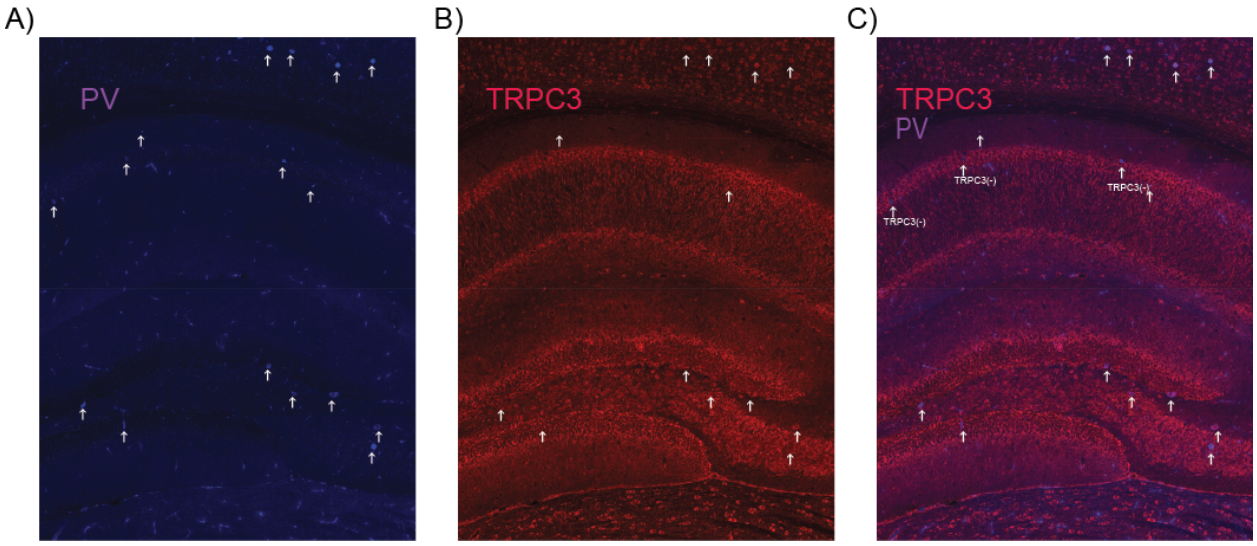

Supplementary Figure 4: TRPC3 is expressed in the majority of parvalbumin positive interneurons that are sparse in pyramidal layer of the hippocampus of wild-type mice. Immunohistochemistry labeling and imaging of **A)** the interneuron marker parvalbumin (PV, purple) and **B)** TRPC3 (red) in the hippocampus of a wild-type mouse. **c)** Representative overlay of the purple and red channels shows some colocalization of PV and TRPC3, but that only sparse numbers of TRPC3+/PV+ interneurons are found in the hippocampus.

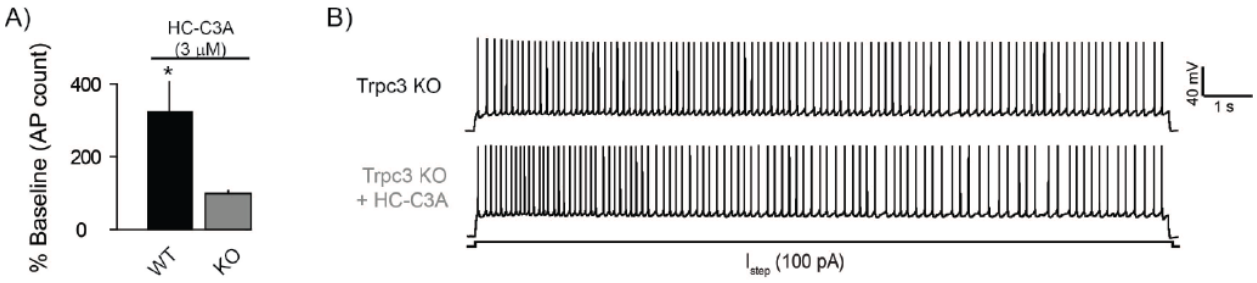

Supplementary Figure 5: TRPC3 antagonist has no effect on hippocampus neurons from Trpc3-/- or intracellular delivery of Trpc3-antibody. (**A**) TRPC3 antagonist HC-C3A has no effect on Hipp neurons lacking TRPC3 protein or when TRPC3 is blocked via intracellular delivery of T TRPC3-antibody (Ab/anti). Step current injections (100 pA, 15 s) were used to evoke firing in ACSF containing pharmacological blockers of ionotropic glutamate and GABA receptors, and again after bath-application of TRPC3 antagonist HC-C3A (3 μM) in brain slices from WT and Trpc3-/- mice or Ab/anti treated neurons. Plot shows blockade of TRPC3 channels with HC-C3A or intracellular TRPC3 Ab for 10 minutes had no effect on firing in neurons (n = 4) from Trpc3-/- mice, indicating that both are specific to TRPC3 and have minimal off-target effects (data pooled and labeled KO; $t(1,9)= -0.35$, $p=0.74$). (**B**) Representative traces illustrate exposure to HC-C3A for 10 minutes had no effect on firing in neurons from *Trpc3* KO group.